Spatiotemporal neural correlates of brain-computer interface learning

Marie-Constance Corsi[a,b,*], Mario Chavez[c], Denis Schwartz[d], Nathalie George[d], Laurent Hugueville[d], Ari E. Khan[e], Sophie Dupont[b], Danielle S. Bassett[e,f,g,h], and Fabrizio De Vico Fallani[a,b]

[a]Inria Paris, Aramis project-team, F-75013, Paris, France

[b]Institut du Cerveau et de la Moelle Epinière, ICM, Inserm, U 1127, CNRS, UMR 7225, Sorbonne Université, F-75013, Paris, France

[c]CNRS, UMR 7225, F-75013, Paris, France

[d]Institut du Cerveau et de la Moelle Epinière, ICM, Inserm U 1127, CNRS UMR 7225, Sorbonne Université, Ecole Normale Supérieure, ENS, Centre MEG-EEG, F-75013, Paris, France

[e]Department of Bioengineering, School of Engineering and Applied Science, University of Pennsylvania, Philadelphia, PA 19104, USA

[f]Department of Neurology, Perelman School of Medicine, University of Pennsylvania, Philadelphia, PA 19104, USA

[g]Department of Physics and Astronomy, College of Arts and Sciences, University of Pennsylvania, Philadelphia, PA 19104, USA

[h]Department of Electrical and Systems Engineering, School of Engineering and Applied Science, University of Pennsylvania, Philadelphia, PA 19104, USA

[*]Corresponding author: Marie-Constance Corsi, Institut du Cerveau et de la Moelle Epinière, 47, boulevard de l'Hôpital, 75013, Paris, France, marie.constance.corsi@gmail.com

November 15, 2018

Abstract

Brain-computer interfaces have been largely developed to allow communication, control, and neurofeedback in human beings. Despite their great potential, BCIs perform inconsistently across individuals. Moreover, the neural processes activated by training that enable humans to achieve good control remain poorly understood. In this study, we show that BCI skill acquisition is paralleled by a progressive reinforcement of task-related activity and by the reduction of connectivity between regions beyond those primarily targeted during the experiments. Notably, these patterns of activity and connectivity reflect growing automaticity and predict future BCI performance. Altogether, our findings provide new insights in the neural mechanisms underlying BCI learning, which have implications for the use of this technology in a broad range of real-life applications.

Introduction

Voluntarily modulating brain activity is a skill that can be learned by capitalizing on the feedback presented to the user. Such an ability is typically used in neurofeedback control to self-regulate putative neural substrates underlying a specific behavior, as well as in brain-machine interfaces, or brain-computer interfaces (BCIs)(1), to directly regulate external devices. Despite the potential impact, from elucidating brain-behavior relationships (2) to identifying new therapeutics for psychiatric (3) and neurological disorders (4; 5), both neurofeedback and BCIs face several challenges that affect their usability. This includes inter-subject variability, uncertain long-term effects, and the apparent failure of some individuals to achieve self-regulation (6). To address this gap, investigators have searched for better decoders of neural activity (7) as well as for psychological factors (8) and appropriate training regimens (9) that can influence user performance. On the other hand, neuroplasticity is thought to be crucial for achieving effective control and this has motivated a deeper understanding of the neurophysiology mechanisms of neurofeedback and BCI learning (10). At small spatial scales, the role of cortico-striatal loops with the associated dopaminergic and glutamatergic synaptic organization has been demonstrated in human and animal studies suggesting the procedural nature of neurofeedback learning (11). At larger spatial scales, evidence supporting the involvement of a distributed network of brain areas related to control, learning, and reward processing has been provided in fMRI-based neurofeedback experiments (12). Recently, a motor imagery (MI) BCI study based on ECoG recordings showed that successful learning was associated with a decreased activity in the dorsal premotor, prefrontal, and posterior parietal cortices (13). To date, however, the emergence of large-scale dynamic cortical activity changes during BCI learning has not been tested directly.

On the above-mentioned grounds, we hypothesized that BCI learning would be paralleled by a dynamic recruitment of a larger network of distributed cortical areas. More specifically, based on previous studies documenting user's transition from a deliberate mental strategy to nearly automatic execution (13; 10), we expected a progressive involvement of task-related regions that are not directly associated with the feedback control. Furthermore, we hypothesized that the characteristics of circuit recruitment in terms of extent, intensity, and inter-regional activity interactions, would be able to predict the success of learning.

To test these predictions, we recorded high-density EEG in a group of naive healthy subjects during a simple MI-based BCI training consisting of 4 sessions over 2 weeks. We derived cortical activity maps by performing source-reconstruction and we studied the longitudinal task-modulated changes in different

frequency bands. We evaluated the evolution of the size and strength of the activated cortical network as well as the functional connectivity between different regions of interest. Finally, we tested their relationships with learning as measured by the BCI performance. See the section entitled *Materials and methods* for a detailed description of the experimental and methodological design.

Results

Behavioral performance

The BCI task consisted of a 1D, two-target right-justified box task (14) in which subjects learned to control the vertical position of a cursor that moves from left to right on the screen. To hit the up-target, subjects performed a motor imagery-based hand grasping (MI condition) and to hit the down-target, they stayed at rest (Rest condition). At the beginning of each experimental session, we identified the controlling EEG features during a calibration phase among the electrodes over the contra-lateral motor area and within the standard α and β frequency ranges (*SI Figure S2*).

We found that the ability to control the BCI significantly increased across sessions (days) but not within sessions (hours) (see *SI Figure S3*). The session effect was also present when we averaged the BCI accuracy scores across the runs of each session (one-way ANOVA, $F_{3,57} = 13.9,\ p = 6.56.10^{-7}$). Despite the expected high inter-subject variability ($> 8.95\%$), (see *SI Table S1*), the group reached on average a reasonable level of control - above the chance level of 57 % (15) - by the end of the training (Figure 1A).

We next investigated the characteristics of the EEG controlling features. From a spatial perspective, the electrodes above the primary motor area of the hand (C3 and CP3) tended to better discriminate the MI and Rest mental states (Figure 1B). The most discriminant frequencies occurred between high-α and low-β ranges (Figure 1B). These results are in line with previous studies (16). Notably, we observed a progressive focus over CP3 and low-β ranges throughout the sessions.

Among the demographical and psychological items that we measured before the experiment (see *SI Materials and methods*), only the kinesthetic imagery score (17) moderately predicted the ability of subjects to control the BCI (Spearman, r = 0.45, p = 0.045). We also found that these items could not predict the evolution of BCI accuracy over time (see *SI Table S2*, non-significant values of the other tests), suggesting that BCI skill acquisition is a complex process that could not be simply explained by a reduced number of scores taken from questionnaires.

Spatiotemporal cortical changes during training

We evaluated the spatiotemporal cortical changes associated with the BCI training by performing a group analysis at the source-space level. Specifically, we computed the task-related brain activity by statistically comparing the power spectra of the MI versus the Rest condition in each session (*Materials and methods*). In both α and β frequency ranges, we found a progressive involvement of distributed sources in the cortical hemisphere contralateral to the movement (Figure 2). The regions that were involved exhibited a significant power decrease ($p < 0.025$), as typically observed during motor-related tasks (18). These decrements were particularly diffuse in the α_2 and β_1 frequency sub-bands, and were more pronounced in the primary somatosensory cortex (pre- and postcentral gyri, central sulcus), the primary motor cortex (inferior and superior parts of the precentral sulcus), the frontal, the prefrontal, the temporal, and the parietal areas.

Notably, the observed decreases tended to focus more on the contralateral pre- and postcentral gyri at the end of training (Figure 2 and *SI table S3*). We did not observe comparable significant differences in the other frequency bands (*SI Figures S4-S6*). To quantify these changes at the individual level, we computed both the size C_S and the relative power Δ_P of the most significant cluster of cortical sources extracted in each subject (*Material and methods*). These quantities exhibited a significant session effect only in the α and β frequency ranges ($p < 0.002$, *SI Table S5*). This result indicates that BCI training is accompanied by an increase of desynchronization (Δ_P) that tends to be more diffuse (C_S) implicating areas that are also outside the sensorimotor cortex.

Notably, the observed longitudinal changes could be explained by the significant decrease of the relative power in the MI condition ($F_{3,57} = 4.82$, $p = 0.003$; $F_{3,57} = 3.09$, $p = 0.024$ respectively in the α_2 and β_1 frequency sub-bands), while the Rest condition did not vary across sessions (α_2) or varied less significantly than the MI condition (β_1) (Figure 3). As expected, this result confirmed that during training, the subjects learned how to imagine the movement rather than to remain at rest.

Functional connectivity network analysis

To evaluate the cortical changes at the network level, we considered functional connectivity (FC) patterns that have been shown to be senstive to BCI-related tasks (19) as well as to learning processes (20). For that purpose, we calculated the imaginary coherence between the source reconstructed signals of each pair of regions of interest (ROIs) corresponding to the Destrieux atlas (*Material and methods*). Imaginary coherence

is a spectral measure of coherence weakly affected by volume conduction and spatial leakage (21; 22).

By statistically comparing the FC values between MI and Rest conditions at the group level, we found a progressive decrease of task-related connectivity in both α and β frequency ranges across sessions. No significant differences were observed in the other frequency bands (Figure 4, SI Figures S9-S10). In α frequency ranges, the strongest decreases involved fronto-occipital (α_1) and parieto-occipital (α_2) interactions. In β frequency ranges, they rather involved fronto-central (β_1) and bilateral temporal interactions (β_2), and to a minor extent bilateral central connectivity (*SI Table S6*). For each subject, we next quantified the regional connectivity changes by computing the relative node strength Δ_N in the α and β frequency ranges (*Materials and methods*). Significant across-session decreases were spatially diffused involving bilaterally frontal, temporal and occipital areas in the α frequency ranges, while in the β frequency ranges the significant decreases were more focused over the right frontal, the left primary motor cortex, the left central, and parietal areas ($p < 0.025$, see *SI Figures S11-S12* and *Table S7*).

Collectively, the results indicate that BCI training is associated with a progressive decrease of functional integration among cortical systems that are specialized for diverse functions.

Predictive neural markers of BCI performance

To better understand how the observed cortical changes in α and β frequency ranges were associated with performance, we conducted a correlation analysis to identify neural features that could explain BCI accuracy in the same session and that could predict BCI accuracy in a future session. In general, the strongest correlations occurred in the α_2 and β_1 frequency bands (see *SI Table S8* and *SI Figure S13*). In these bands, both power and connectivity metrics correlated significantly with performance within the same session. Higher BCI scores were associated with the recruitment of a higher number of task-related cortical sources C_S (in α_2, $r = 0.49$, $p = 0.004$, Figure 5A and see *SI Table S8* for β_1) and with larger decreases of relative power Δ_P (in α_2, $r = -0.54$, $p = 0.003$, Figure 5B and see *SI Table S8* for β_1). A better performance was also associated with a decrease in regional connectivity decrease (*SI Figure S13*). In particular, we found strong correlations distributed across occipital, pre-supplementary motor, and frontal cortices in the α_2 band (Δ_N, Figure 5C).

Power changes in α_2 and β_1 frequency bands were not only associated with performance within the same training session but also predicted, with similar trends, the BCI accuracy in the subsequent session (in C_S, $r = 0.37$, $p = 0.004$, Figure 5A, and *SI Table S8*; Δ_P, $r = -0.53$, $p = 1.35.10^{-5}$ for α_2, Figure 5

B, see *SI Table S8* for β_1). In terms of regional connectivity, we also found significant predictions (*SI Figure S13*). This was particularly evident in the α_2 band where the connectivity decrease in the frontal and temporal (superior temporal gyrus) areas was associated with better future performance (Δ_N, Figure 5C).

Altogether, these findings demonstrate that the observed dynamic cortical changes are intrinsically associated with successful BCI learning.

Discussion

Neuroplasticity and learning

Identifying the large-scale neural mechanisms underlying plasticity is fundamental to understand human learning (20). The ability to voluntarily modulate neural activity to control a BCI appears to be a learned skill. Investigators have repeatedly documented that task performance typically increases over the course of practice (23; 24), while BCI users often report transitioning from a deliberate cognitive strategy (e.g. MI) to a nearly automatic goal-directed approach focused directly on effector control. This evidence is indicative of a learning process taking place in the brain that is consistent with procedural motor learning.

Efforts in understanding the neural dynamics underlying BCI skill acquisition have been made by using neuroimaging techniques in primates (23; 25) as well as in humans (26; 27). Results indicated that even if the use of a BCI only requires the activity modulation of a motor-related brain area, a dynamic and distributed network of remote cortical areas is involved in the early acquisition of BCI proficiency within the same session. However, how such a network evolves over longer time-scales of BCI training is still relatively unknown.

Here, we showed that a BCI training performed across several days elicits a reinforcement of power desynchronization of the sensorimotor areas that is paralleled by a progressive decrease of functional integration between differently specialized cortical regions. Notably, regional connectivity tended to decrease more for associative areas in the α frequency ranges, while connectivity decrements were more important for motor-related regions in the β frequency ranges (see *SI Figures S11-S12, Table S7*). Notably, these cortical systems are known to play a crucial role in motor sequence learning and in abstract task learning (28; 29; 30; 31).

Prediction of performance

Forecasting behavior is one of the main challenges for many real-life situations, from econometry to epidemiology. In the BCI context, a correct prognosis will allow an appropriate identification of neural features, and thus, an effective skill acquisition. Investigators have recognized the need for co-adaptive BCI architectures that accommodate the dynamic nature of the neural features used as inputs (32). Notably, FC-based features have recently been posited as potential alternatives to univariate features (33) (e.g. power spectra); in some cases, such FC features are correlated with the user's performance, suggesting their potential in improving MI-based BCI accuracy (34). Besides, several studies have started to take into account psychological (e.g. anxiety) or demographical items to predict BCI performances. However, the associated results seem to be contradictory (35; 36; 37). It has become apparent that there is a critical need for biologically informed computational models and theory to characterize the neural mechanisms of BCI learning and to predict future performance, thereby enabling the generalization of these results across subject cohorts, and the optimization of BCI architectures for individual users (38).

In this work, the modulation of brain activity and functional connectivity in the α and β frequency bands by the BCI training was evident. The number of regions involved in the task, the associated power desynchronization and connectivity decrease in each participant could be used to predict that participant's ability to control a BCI. More importantly, the same cortical changes could forecast the future amount of learning as measured by the BCI accuracy in the subsequent session. This result could potentially be used to inform decisions on how to train individuals depending on the current neural properties of their brain.

BCI "illiteracy"

BCIs are increasingly used for control and communication as well as for the treatment of neurological diseases (39). While performance usually reaches high levels of accuracy (around 90 %), a non-negligible portion of users (between 15 % and 30 %) exhibit an inability to communicate with a BCI (40). This is a well-known phenomenon that is informally referred as to "BCI illiteracy". Critically, BCI illiteracy affects the usability of BCIs in the user's daily life (41) but the reasons (42; 43) and even the definition for such inability (44) is still under debate. On the one hand, different approaches have been proposed to solve the problem by improving feature extraction and decoding algorithms (32), combining different modalities (45), or taking into account the user's profile (43). On the other hand, alternative accuracy metrics based on the separability of brain features, rather than on the simple count of successful control, have been shown

to be more relevant for the proof-of-existence of subject's learning (46). Our results show that a functional reorganization of the cortical activity is taking place during BCI training. These findings suggest that BCI illiteracy could be an epiphenomenon biased by the nature of standard performance metrics which are affected by decoder recalibration (47), re-parameterizations of the BCI, and the application and adoption of better mental strategies (48; 49), among other factors. It is possible that other metrics, integrating both real performance and functional brain changes should be taken into account to better assess individual learning (46).

Limitations

We considered high-density EEG to quantify the dynamic changes related to BCI training. While scalp-EEG offers a unique temporal resolution (on the order of milliseconds) to study oscillatory neural changes at different frequencies, it suffers from a low spatial resolution (50). Although we performed source-reconstruction to estimate the cortical activity, evaluating the role of subcortical areas which are known to play a fundamental role in human learning remains challenging (51). More studies, involving multimodal neuroimaging techniques (e.g., fMRI and EEG (52)), are therefore needed to reveal the neural changes associated with BCI training at a finer spatial scale.

The temporal window of two weeks considered in our experiment prevents us from observing behavioral and neural changes over longer timescales and therefore, might not be sufficient to observe the full learning process (53). Here, BCI skill acquisition was paralleled by a progressive focused activity over the sensorimotor areas together with a loss of large-scale connectivity, together indicating the initiation of an automaticity process typical of procedural motor learning (54). Future studies are necessary to assess whether and how the observed cortical patterns will evolve with longer BCI training. While the BCI accuracy was highly variable across individuals, the group-averaged performance was relatively low as compared to the state-of-the-art (55). It is important to mention that the main goal of the present work was not to maximize the performance but to study the neural mechanisms underlying BCI learning. In this respect, all our experimental subjects were BCI-naive and exhibited on average an increase of performance reflecting a successful BCI skill acquisition. From this work alone, we are unable to determine whether or not learning is the only possible modulator of the observed cortical changes. While no correlation has been found with behavioral factors (i.e. anxiety), complementary experiments could be designed to test whether the observed cortical changes are also modulated by fatigue or exogenous stimulants to increase motor excitability (i.e.,

transcranial direct current stimulation, tDCS (56)).

Conclusion

Consistent with our hypothesis, we have identified specific cortical changes that characterize dynamic brain reorganization during BCI training. The progressive enhancement of task-modulated activity in motor-related areas, together with the fading of distributed functional connectivity, are significantly associated with BCI learning. These cortical signatures varied over individuals and, more importantly, were significant predictors of future BCI performance. Taken together, our results offer new insights into the crucial role of neuroplasticity in the prediction of human learning.

Material and methods

Participants and experiment

Twenty healthy subjects (aged 27.45 $\pm$ 4.01 years, 12 men), all right-handed, participated in the study. Subjects were enrolled in a longitudinal EEG-based BCI training (twice a week for two weeks, *SI text*). All subjects were BCI-naive and none presented with medical or psychological disorders. According to the declaration of Helsinki, written informed consent was obtained from subjects after explanation of the study, which was approved by the ethical committee CPP-IDF-VI of Paris. All participants received financial compensation at the end of their participation. The BCI task consisted of a standard 1D, two-target box task (14) in which the subjects modulated their α [8-12 Hz] and/or β [14-29 Hz] activity to control the vertical position of a cursor moving with constant velocity from the left to the right side of the screen. To hit the target-up, the subjects performed a sustained motor imagery of their right-hand grasping (MI condition) and to hit the target-down they remained at rest (Rest condition). Each trial lasted 7 s and consisted of a 1 s of inter-stimulus, followed by 2 s of target presentation, 3 s of feedback and 1 s of result presentation. BCI control features (EEG electrode and frequency) were selected in a calibration phase at the beginning of each session, by instructing the subjects to perform the BCI tasks without any visual feedback (*SI Text, SI Figure 2)*.

Experiments were conducted with a 74 EEG-channel system, with Ag/AgCl sensors (Easycap, Germany) placed according to the standard 10-10 montage. EEG signals were referenced to mastoid signals, with the

ground electrode located at the left scapula, and impedances were kept lower than 20 kOhms. EEG data were recorded in a shielded room with a sampling frequency of 1 kHz and a bandwidth of 0.01-300 Hz. The subjects were seated in front of a screen at a distance of 90 cm. To ensure the stability of the position of the hands, the subjects rested their arms on a comfortable support, with palms facing upward. We also recorded electromyogram (EMG) signals from the left and right arm of subjects. Expert bioengineers visually inspected EMG activity to ensure that subjects were not moving their forearms during the recording sessions. We carried out BCI sessions with EEG signals transmitted to the BCI2000 toolbox (57) via the Fieldtrip buffer (58).

EEG preprocessing and source reconstruction

The signals were downsampled to 250 Hz before performing an ICA (Independent Components Analysis) with the Infomax approach using the Fieldtrip toolbox (59; 58). The number of computed components corresponds to the number of channels, i.e. 72 (T9 and T10 were removed). Only the independent components (ICs) that contain ocular or cardiac artifacts were removed. The selection of the components was performed via a visual inspection of the signals (from both time series and topographies). On average, 2 ICs were removed. Data were then segmented into epochs of seven seconds corresponding to the trial period. Our quality check was based on the variance and the visual inspection of the signals. For each channel and each trial, we plotted the associated variance values. We kept a ratio below 3 between the noisiest and the cleanest trials. The percentage of removed trials was kept below 10 % of the total number of trials (60).

After having average referenced signals, we performed source reconstruction by computing the individual head model with the Boundary Element Method (BEM) (61; 62). BEM surfaces were obtained from three layers associated with the subject's MRI (scalp, inner skull, outer skull) that contain 1922 vertices each. Then, we estimated the sources with the weighted Minimum Norm Estimate (wMNE) (63; 64; 65) via the Brainstorm toolbox (66). Here, we used the identity matrix as the noise covariance matrix. The minimum norm estimate corresponds in our case to the current density map. We constrained the dipole orientations normal to the cortex. To perform the group analysis, we projected the sources estimated on each subject, and each session, onto the common template anatomy MNI-ICBM152 (67) via Shepard's interpolation. From these signals, we computed the associated power spectra. To identify the anatomical structures associated with the obtained clusters without restricting our work on motor or sensorimotor areas, we used the Destrieux atlas (68).

Metrics and statistics

To take into account the subjects' specificity (69), we used a definition of the α and β sub-bands that rely on the Individual Alpha Frequency (IAF) obtained from a resting-state recording that lasted 3 minutes with the subjects' eyes open). Similarly to (70), the IAF corresponds to the first peak obtained between 6 and 12 Hz. The α_1 ranges from IAF - 2 to IAF, α_2 from IAF to IAF + 2, β_1 from IAF + 2 to IAF + 11 and β_2 from IAF + 11 to IAF + 20. For each subject, session, and trial in the source space, we computed the power spectra. We used the Welch method with a window length of 1 s and a window overlap ratio of 50 % applied during the feedback period that ranges from t = 3 s to t = 6 s). In the case of the group analysis presented in Figure 2, we worked within the ICBM152-MNI template. Elsewhere, we used the individual anatomical space. To perform the analysis presented in Figure 2, we computed statistical differences among activations recorded in the MI and the rest conditions at the group level or at the subject level via a paired t-test. Since we expected a desynchronization between the two conditions, we applied a one-tailed t-test. Statistics were corrected for multiple comparisons using the cluster approach (58; 66). We fixed the statistical threshold to 0.05, a minimum number of neighbors of 2 and a number of randomization of 500. Clustering was performed on the basis of spatial adjacency. Cluster-level statistics are obtained by using the sum of the t-values within every cluster. To obtain the relative power Δ_P, we computed the relative difference, in terms of power spectra, between the two conditions, as follows: $\Delta_P = 100 \times \frac{P_{MI}-P_{Rest}}{P_{Rest}}$, where P_{MI} and P_{Rest} correspond, respectively to the averaged power calculated across the cluster from MI and Rest trials. The cluster size C_S was obtained by estimating the number of elements that belong to the cluster that presented the best discrimination between the conditions. To perform the study for each condition separately (Figure 3), we normalized the power spectra with respect to the inter-stimulus interval (ISI) via the Hilbert transform similar to that approach reported in Ref. (27). The connectivity analysis (Figure 4) was based on the cross-spectral estimation computed with the Welch method. To reduce the dimensionality, we extracted the first principal component obtained from the power spectra calculated across the dipoles within each ROI. Then, we computed the imaginary coherence between each pair of ROIs based on the definition proposed in Ref.(22). From the resulting connectivity matrix, we next computed the relative node strength Δ_N similarly to what we did for the relative power. The strength of the i-th node was here calculated by summing the values of the i-th row of the connectivity matrix.

0.1 Data availability

The data that support the findings of this study are available from the corresponding author upon

References

[1] McFarland, D. J. & Wolpaw, J. R. Brain–computer interface use is a skill that user and system acquire together. *PLOS Biology* **16**, e2006719 (2018). URL https://journals.plos.org/plosbiology/article?id=10.1371/journal.pbio.2006719.

[2] Shibata, K., Watanabe, T., Sasaki, Y. & Kawato, M. Perceptual Learning Incepted by Decoded fMRI Neurofeedback Without Stimulus Presentation. *Science* **334**, 1413–1415 (2011). URL https://doi.org/10.1126%2Fscience.1212003.

[3] Kim, S. & Birbaumer, N. Real-time functional MRI neurofeedback. *Current Opinion in Psychiatry* **27**, 332–336 (2014). URL https://doi.org/10.1097%2Fyco.0000000000000087.

[4] Pichiorri, F. *et al.* Brain-computer interface boosts motor imagery practice during stroke recovery. *Annals of Neurology* **77**, 851–865 (2015). URL https://doi.org/10.1002%2Fana.24390.

[5] King, C. E., Wang, P. T., Chui, L. A., Do, A. H. & Nenadic, Z. Operation of a brain-computer interface walking simulator for individuals with spinal cord injury. *Journal of NeuroEngineering and Rehabilitation* **10**, 77 (2013). URL https://doi.org/10.1186%2F1743-0003-10-77.

[6] Vidaurre, C. & Blankertz, B. Towards a Cure for BCI Illiteracy. *Brain Topography* **23**, 194–198 (2009). URL https://doi.org/10.1007%2Fs10548-009-0121-6.

[7] Lotte, F. *et al.* A review of classification algorithms for EEG-based brain–computer interfaces: a 10 year update. *Journal of Neural Engineering* **15**, 031005 (2018). URL https://doi.org/10.1088%2F1741-2552%2Faab2f2.

[8] Kleih, S., Nijboer, F., Halder, S. & Kübler, A. Motivation modulates the P300 amplitude during brain–computer interface use. *Clinical Neurophysiology* **121**, 1023–1031 (2010). URL https://doi.org/10.1016%2Fj.clinph.2010.01.034.

[9] Jeunet, C., Jahanpour, E. & Lotte, F. Why standard brain-computer interface (BCI) training protocols

should be changed: an experimental study. *Journal of Neural Engineering* **13**, 036024 (2016). URL https://doi.org/10.1088%2F1741-2560%2F13%2F3%2F036024.

[10] Sitaram, R. *et al.* Closed-loop brain training: the science of neurofeedback. *Nature Reviews Neuroscience* **18**, 86–100 (2016). URL https://doi.org/10.1038%2Fnrn.2016.164.

[11] Koralek, A. C., Jin, X., II, J. D. L., Costa, R. M. & Carmena, J. M. Corticostriatal plasticity is necessary for learning intentional neuroprosthetic skills. *Nature* **483**, 331–335 (2012). URL https://doi.org/10.1038%2Fnature10845.

[12] Emmert, K. *et al.* Meta-analysis of real-time fMRI neurofeedback studies using individual participant data: How is brain regulation mediated? *NeuroImage* **124**, 806–812 (2016). URL https://doi.org/10.1016%2Fj.neuroimage.2015.09.042.

[13] Wander, J. D. *et al.* Distributed cortical adaptation during learning of a brain-computer interface task. *Proceedings of the National Academy of Sciences* **110**, 10818–10823 (2013). URL https://doi.org/10.1073%2Fpnas.1221127110.

[14] Wolpaw, J. R., McFarland, D. J., Vaughan, T. M. & Schalk, G. The Wadsworth Center brain-computer interface (BCI) research and development program. *IEEE Transactions on Neural Systems and Rehabilitation Engineering* **11**, 204–207 (2003).

[15] Müller-putz, G. R., Scherer, R., Brunner, C., Leeb, R. & Pfurtscheller, G. Better than random: a closer look on BCI results. *International Journal of Bioelectromagnetism* **10** (2008).

[16] Neuper, C. & Pfurtscheller, G. Event-related dynamics of cortical rhythms: frequency-specific features and functional correlates. *International Journal of Psychophysiology* **43**, 41–58 (2001).

[17] Roberts, R., Callow, N., Hardy, L., Markland, D. & Bringer, J. Movement imagery ability: development and assessment of a revised version of the vividness of movement imagery questionnaire. *Journal of Sport and Exercise Psychology* **30**, 200–221 (2008).

[18] Lopes da Silva, F. EEG and MEG: Relevance to Neuroscience. *Neuron* **80**, 1112–1128 (2013). URL http://www.sciencedirect.com/science/article/pii/S0896627313009203.

[19] Mottaz, A. *et al.* Modulating functional connectivity after stroke with neurofeedback: Effect on motor deficits in a controlled cross-over study. *Neuroimage: Clinical* **20**, 336–346 (2018). URL https://www.ncbi.nlm.nih.gov/pmc/articles/PMC6091229/.

[20] Bassett, D. S. & Khambhati, A. N. A network engineering perspective on probing and perturbing cognition with neurofeedback. *Annals of the New York Academy of Sciences* **1396**, 126–143 (2017). URL https://www.ncbi.nlm.nih.gov/pmc/articles/PMC5446287/.

[21] Nolte, G. *et al.* Identifying true brain interaction from EEG data using the imaginary part of coherency. *Clinical Neurophysiology* **115**, 2292–2307 (2004).

[22] Sekihara, K., Owen, J., Trisno, S. & Nagarajan, S. S. Removal of spurious coherence in MEG source-space coherence analysis. *IEEE transactions on bio-medical engineering* **58**, 3121–3129 (2011). URL https://www.ncbi.nlm.nih.gov/pmc/articles/PMC4096348/.

[23] Ganguly, K. & Carmena, J. Emergence of a stable cortical map for neuroprosthetic control. *PLoS Biology* **7**, e1000153 (2009).

[24] Moritz, C., Perlmutter, S. & Fetz, E. Direct control of paralysed muscles by cortical neurons. *Nature* **456**, 639–42 (2008).

[25] Carmena, J. *et al.* Learning to control a brain-machine interface for reaching and grasping by primates. *PLoS Biology* **1**, E42 (2003).

[26] Pichiorri, F. *et al.* Sensorimotor rhythm-based brain–computer interface training: the impact on motor cortical responsiveness. *Journal of Neural Engineering* **8**, 025020 (2011). URL https://doi.org/10.1088%2F1741-2560%2F8%2F2%2F025020.

[27] Wander, J. D. *et al.* Distributed cortical adaptation during learning of a brain–computer interface task. *Proceedings of the National Academy of Sciences* **110**, 10818–10823 (2013). URL http://www.ncbi.nlm.nih.gov/pmc/articles/PMC3696802/.

[28] McDougle, S. D., Ivry, R. B. & Taylor, J. A. Taking Aim at the Cognitive Side of Learning in Sensorimotor Adaptation Tasks. *Trends in Cognitive Sciences* **20**, 535–544 (2016).

[29] Hétu, S. *et al.* The neural network of motor imagery: an ALE meta-analysis. *Neuroscience & Biobehavioral Reviews* **37**, 930–949 (2013).

[30] Hardwick, R. M., Caspers, S., Eickhoff, S. B. & Swinnen, S. P. Neural correlates of action: Comparing meta-analyses of imagery, observation, and execution. *Neuroscience & Biobehavioral Reviews* **94**, 31–44 (2018). URL http://www.sciencedirect.com/science/article/pii/S0149763417309284.

[31] Dayan, E. & Cohen, L. G. Neuroplasticity Subserving Motor Skill Learning. *Neuron* **72**, 443–454 (2011). URL https://doi.org/10.1016%2Fj.neuron.2011.10.008.

[32] Vidaurre, C., Sannelli, C., Müller, K.-R. & Blankertz, B. Co-adaptive calibration to improve BCI efficiency. *Journal of Neural Engineering* **8**, 025009 (2011).

[33] Krusienski, D. J., McFarland, D. J. & Wolpaw, J. R. Value of amplitude phase, and coherence features for a sensorimotor rhythm-based brain–computer interface. *Brain Research Bulletin* **87**, 130–134 (2012). URL https://doi.org/10.1016%2Fj.brainresbull.2011.09.019.

[34] Sugata, H. *et al.* Alpha band functional connectivity correlates with the performance of brain-machine interfaces to decode real and imagined movements. *Frontiers in Human Neuroscience* **8** (2014). URL https://doi.org/10.3389%2Ffnhum.2014.00620.

[35] Neuper, C., Scherer, R., Wriessnegger, S. & Pfurtscheller, G. Motor imagery and action observation: Modulation of sensorimotor brain rhythms during mental control of a brain–computer interface. *Clinical Neurophysiology* **120**, 239–247 (2009). URL http://www.sciencedirect.com/science/article/pii/S1388245708012601.

[36] Hammer, E. M. *et al.* Psychological predictors of SMR-BCI performance. *Biological Psychology* **89**, 80–86 (2012).

[37] Vuckovic, A. & Osuagwu, B. A. Using a motor imagery questionnaire to estimate the performance of a Brain-Computer Interface based on object oriented motor imagery. *Clinical Neurophysiology* **124**, 1586–1595 (2013).

[38] Perdikis, S., Leeb, R. & Millán, J. d. R. Subject-oriented training for motor imagery brain-computer interfaces. *Conf Proc IEEE Engineering in Medicine and Biology Society* **2014**, 1259–1262 (2014).

[39] Clerc, M., Bougrain, L. & Lotte, F. (eds.) *Brain-Computer Interfaces 2* (John Wiley & Sons Inc., 2016). URL https://doi.org/10.1002%2F9781119332428.

[40] Allison, B. Z. & Neuper, C. Could Anyone Use a BCI? In Tan, D. S. & Nijholt, A. (eds.) *Brain-Computer Interfaces*, Human-Computer Interaction Series, 35–54 (Springer London, 2010). URL http://link.springer.com/chapter/10.1007/978-1-84996-272-8_3.

[41] Claudia Zickler, V. K. A. A.-K. S. K. A. K. M. M. D. M. S. M. C. N. M. R. R. R. P. S.-S. E.-J. H., Valentina Di Donna. BCI Applications for People with Disabilities: Defining User Needs and

User Requirements (2009). URL http://ebooks.iospress.nl/publication/916. Accessed on Tue, September 18, 2018.

[42] Blankertz, B. *et al.* Neurophysiological predictor of SMR-based BCI performance. *NeuroImage* **51**, 1303–1309 (2010). URL http://www.sciencedirect.com/science/article/pii/S1053811910002922.

[43] Jeunet, C., N'Kaoua, B., Subramanian, S., Hachet, M. & Lotte, F. Predicting Mental Imagery-Based BCI Performance from Personality, Cognitive Profile and Neurophysiological Patterns. *PLoS ONE* **10**, e0143962 (2015).

[44] Thompson, M. C. Critiquing the Concept of BCI Illiteracy. *Science and Engineering Ethic* (2018). URL https://doi.org/10.1007/s11948-018-0061-1.

[45] Müller-Putz, G. *et al.* Towards Noninvasive Hybrid Brain-Computer Interfaces: Framework, Practice, Clinical Application and Beyond. *Proceedings of the IEEE* **103**, 926–943 (2015).

[46] Perdikis, S., Tonin, L., Saeedi, S., Schneider, C. & Millán, J. d. R. The Cybathlon BCI race: Successful longitudinal mutual learning with two tetraplegic users. *PLoS Biology* **16** (2018). URL https://www.ncbi.nlm.nih.gov/pmc/articles/PMC5944920/.

[47] Perdikis, S., Leeb, R. & d R Millán, J. Context-aware adaptive spelling in motor imagery BCI. *Journal of Neural Engineering* **13**, 036018 (2016). URL https://doi.org/10.1088%2F1741-2560%2F13%2F3%2F036018.

[48] Kober, S. E., Witte, M., Ninaus, M., Neuper, C. & Wood, G. Learning to modulate one's own brain activity: the effect of spontaneous mental strategies. *Frontiers in Human Neuroscience* **7** (2013). URL https://doi.org/10.3389%2Ffnhum.2013.00695.

[49] Perdikis, S., Leeb, R. & Millan, J. D. R. Subject-oriented training for motor imagery brain-computer interfaces. In *2014 36th Annual International Conference of the IEEE Engineering in Medicine and Biology Society* (IEEE, 2014). URL https://doi.org/10.1109%2Fembc.2014.6943826.

[50] da Silva, F. L. EEG and MEG: Relevance to Neuroscience. *Neuron* **80**, 1112–1128 (2013). URL https://doi.org/10.1016%2Fj.neuron.2013.10.017.

[51] Krishnaswamy, P. *et al.* Sparsity enables estimation of both subcortical and cortical activity from MEG and EEG. *Proceedings of the National Academy of Sciences* **114**, E10465–E10474 (2017). URL https://doi.org/10.1073%2Fpnas.1705414114.

[52] Perronnet, L. *et al.* Unimodal Versus Bimodal EEG-fMRI Neurofeedback of a Motor Imagery Task. *Frontiers in Human Neuroscience* **11** (2017). URL https://doi.org/10.3389%2Ffnhum.2017.00193.

[53] Yin, H. H. *et al.* Dynamic reorganization of striatal circuits during the acquisition and consolidation of a skill. *Nature Neuroscience* **12**, 333–341 (2009). URL https://www.ncbi.nlm.nih.gov/pmc/articles/PMC2774785/.

[54] Seger, C. A. & Miller, E. K. Category Learning in the Brain. *Annual Review of Neuroscience* **33**, 203–219 (2010). URL https://www.ncbi.nlm.nih.gov/pmc/articles/PMC3709834/.

[55] Vidaurre, C. & Blankertz, B. Towards a Cure for BCI Illiteracy. *Brain Topography* **23**, 194–198 (2010). URL http://www.ncbi.nlm.nih.gov/pmc/articles/PMC2874052/.

[56] Nitsche, M. A. *et al.* Facilitation of Implicit Motor Learning by Weak Transcranial Direct Current Stimulation of the Primary Motor Cortex in the Human. *Journal of Cognitive Neuroscience* **15**, 619–626 (2003). URL https://doi.org/10.1162%2F089892903321662994.

[57] Schalk, G., McFarland, D. J., Hinterberger, T., Birbaumer, N. & Wolpaw, J. R. BCI2000: a general-purpose brain-computer interface (BCI) system. *IEEE Transactions on Biomedical Engineering* **51**, 1034–1043 (2004).

[58] Oostenveld, R. *et al.* FieldTrip: Open Source Software for Advanced Analysis of MEG, EEG, and Invasive Electrophysiological Data, FieldTrip: Open Source Software for Advanced Analysis of MEG, EEG, and Invasive Electrophysiological Data. *Computational Intelligence and Neuroscience, Computational Intelligence and Neuroscience* **2011, 2011**, e156869 (2010). URL http://www.hindawi.com/journals/cin/2011/156869/abs/,http://www.hindawi.com/journals/cin/2011/156869/abs/.

[59] Bell, A. J. & Sejnowski, T. J. An information-maximization approach to blind separation and blind deconvolution. *Neural Computation* **7**, 1129–1159 (1995).

[60] Gross, J. *et al.* Good practice for conducting and reporting MEG research. *Neuroimage* **65**, 349–363 (2013).

[61] Fuchs, M., Wagner, M. & Kastner, J. Boundary element method volume conductor models for EEG source reconstruction. *Clinical Neurophysiology* **112**, 1400–1407 (2001). URL http://www.sciencedirect.com/science/article/pii/S1388245701005892.

[62] Gramfort, A., Papadopoulo, T., Olivi, E. & Clerc, M. OpenMEEG: opensource software for quasistatic

bioelectromagnetics. *BioMedical Engineering OnLine* **9**, 45 (2010). URL http://dx.doi.org/10.1186/1475-925X-9-45.

[63] Fuchs, M., Wagner, M., Köhler, T. & Wischmann, H. A. Linear and nonlinear current density reconstructions. *Journal of Clinical Neurophysiology* **16**, 267–295 (1999).

[64] Lin, F.-H. *et al.* Assessing and improving the spatial accuracy in MEG source localization by depth-weighted minimum-norm estimates. *Neuroimage* **31**, 160–171 (2006).

[65] Gramfort, A. *et al.* MNE software for processing MEG and EEG data. *Neuroimage* **86**, 446–460 (2014).

[66] Tadel, F., Baillet, S., Mosher, J., Pantazis, D. & Leahy, R. Brainstorm: A User-Firendly Application for MEG/EEG Analysis. *Computational Intelligence and Neuroscience* **2011** (2011). URL http://dx.doi.org/10.1155/2011/879716.

[67] Mazziotta, J. *et al.* A Four-Dimensional Probabilistic Atlas of the Human Brain. *Journal of the American Medical Informatics Association* **8**, 401–430 (2001). URL https://www.ncbi.nlm.nih.gov/pmc/articles/PMC131040/.

[68] Destrieux, C., Fischl, B., Dale, A. & Halgren, E. Automatic parcellation of human cortical gyri and sulci using standard anatomical nomenclature. *Neuroimage* **53**, 1–15 (2010). URL https://www.ncbi.nlm.nih.gov/pmc/articles/PMC2937159/.

[69] Klimesch, W. EEG alpha and theta oscillations reflect cognitive and memory performance: a review and analysis. *Brain Research Reviews* **29**, 169–195 (1999). URL http://www.sciencedirect.com/science/article/pii/S0165017398000563.

[70] Pichiorri, F. *et al.* Brain-computer interface boosts motor imagery practice during stroke recovery. *Annals of Neurology* **77**, 851–865 (2015).

Acknowledgments

This work was partially supported by French program "Investissements d'avenir" ANR-10-IAIHU-06; "ANR-NIH CRCNS" ANR-15-NEUC-0006-02 and by NICHD 1R01HD086888-01. The funders had no role in study design, data collection and analysis, decision to publish, or preparation of the manuscript. This work was performed on a platform of France Life Imaging network partly funded by the grant "ANR-11-INBS-0006".

Authors contributions

MC, DS, NG, LH, SD, DSB and FDVF initiated research; MCC, MC, DS, LH, DSB and FDVF designed research; MCC, DS and LH performed research; MCC, DS, LH and AEK contributed analytic tools; MCC and AEK analyzed data; and MCC, DSB, and FDVF wrote the paper. All authors revised and approved the manuscript.

Additional Information

Supplementary Information accompanies this paper.

Figures

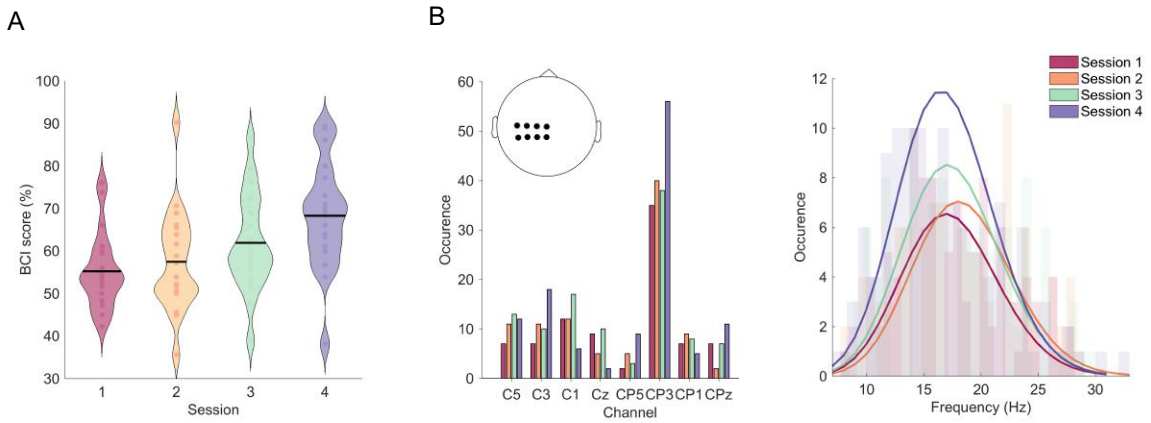

Figure 1: (A) Session effect associated with BCI scores. Each session consists of 6 runs of 32 trials each. Here, we computed the averaged BCI performance across the sessions for each subject. In the violin plots, the black line corresponds to the mean value obtained across the subjects and the outer shape represents the distribution of the BCI scores. (B) Representation of the selected features over all subjects. On the left, we show occurrences obtained across the subjects and the sessions in terms of pre-selected channels; on the right, we show occurrences in terms of frequency bins obtained over the sessions.

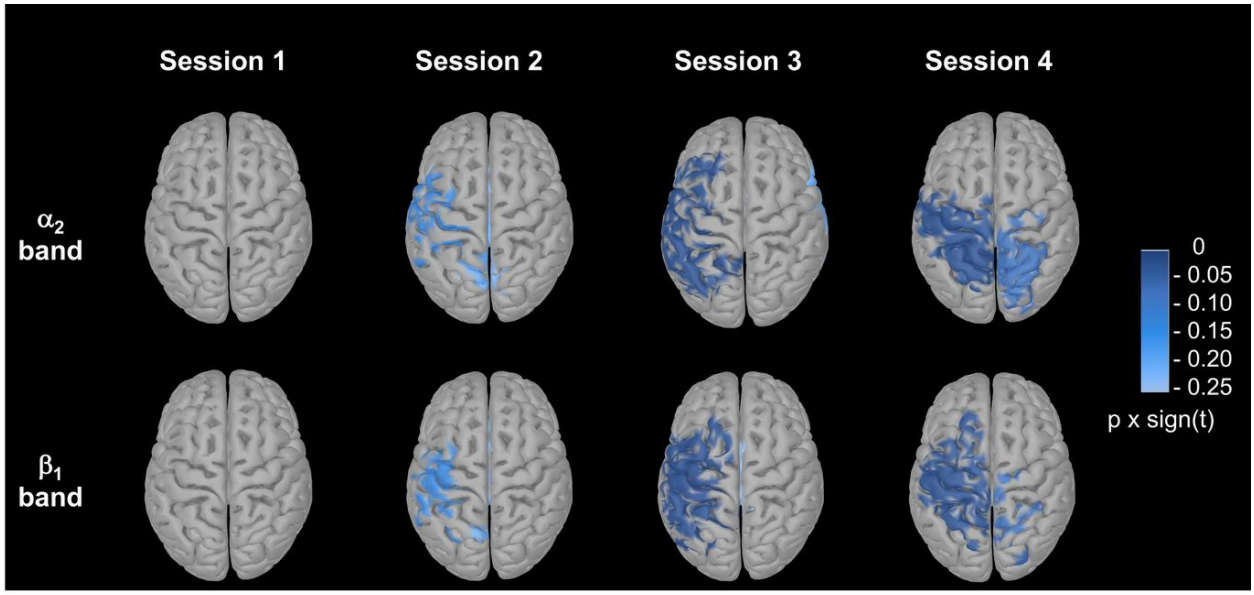

Figure 2: Contrast maps between motor-imagery and rest conditions. Cluster-based permutation results in the α_2 (on the top) and β_1 frequency bands (on the bottom) computed from the group analysis performed across the 20 subjects within the MNI template. Here, we plotted the obtained p-values multiplied by the sign of the t-values resulting from the paired t-test (*Material and methods*).

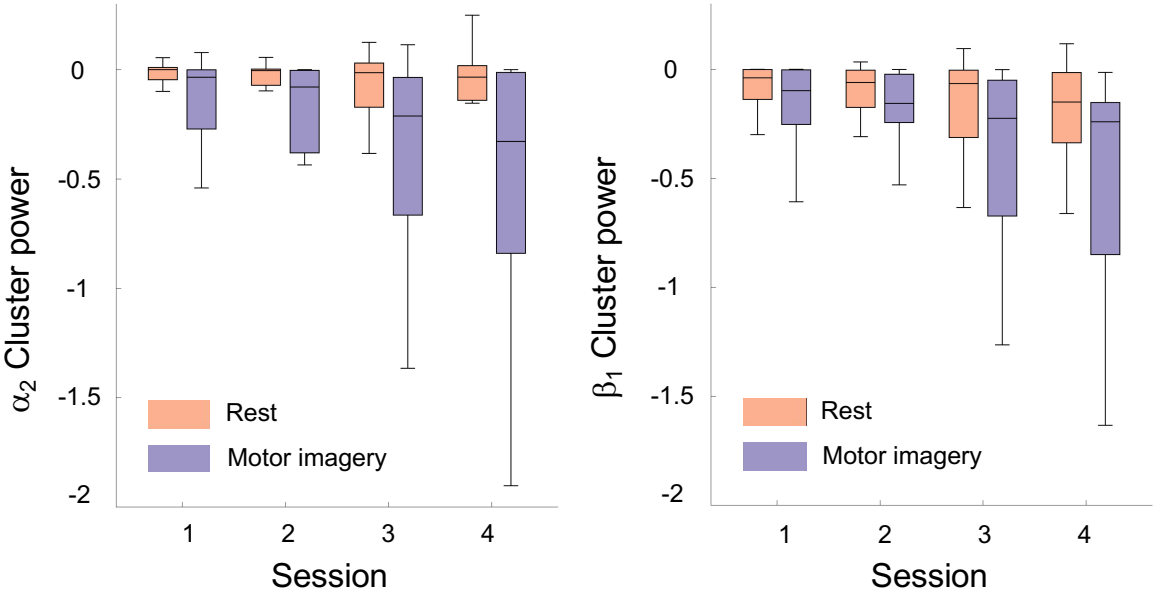

Figure 3: Evolution of the power spectra across the sessions for the motor-imagery and the rest conditions. On the left, the boxplots are associated with the α_2 frequency band and on the right the boxplots are associated with the β_1 frequency band.

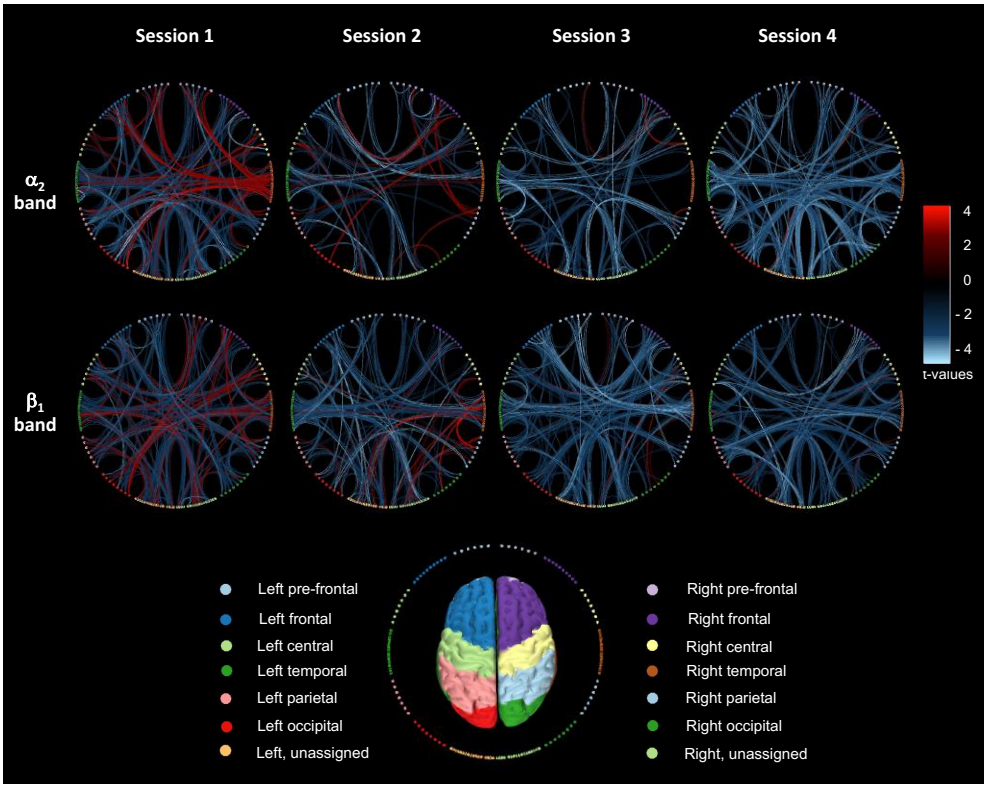

Figure 4: Cortical connectivity changes in BCI training. Results are represented on a circular graph where nodes correspond to different regions of interest (ROIs) and links code the statistical values resulting from two-tailed paired t-test performed between the motor-imagery and rest conditions ($p < 0.005$).The color of each node, corresponds to a specific macro-area as provided by the Brainstorm software; "unassigned" labels mean that the ROI cannot be properly attributed to a specific macro-area *SI Tables S6 and S7*.

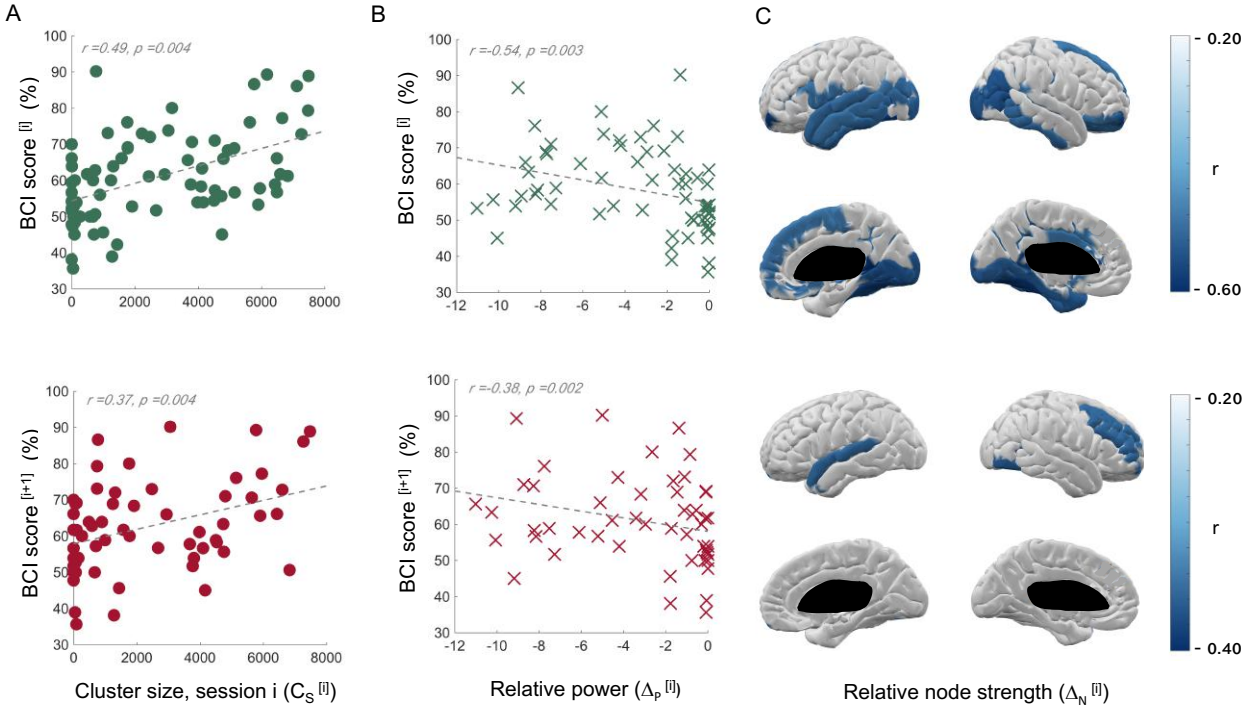

Figure 5: Correlation with BCI performance and prediction of future scores (α_2 band). Figures along the first row correspond to the correlations between the BCI scores of a given session i, $BCI^{[i]}$, and the cluster size $C_S^{[i]}$, the relative power $\Delta_P^{[i]}$ and the relative node strength $\Delta_N^{[i]}$ from the same session i. Figures along the second row correspond to the prediction of the BCI scores of the next session i+1, $BCI^{[i+1]}$, obtained by taking into account, respectively, the cluster size $C_S^{[i]}$, the relative power $\Delta_P^{[i]}$ and the relative node strength $\Delta_N^{[i]}$ from the session i. The r values correspond to the Spearman correlation coefficients, FDR-corrected for multiple comparison ($p < 0.05$). For a detailed account of these results, see *SI Table S6* and *Figure S14*.